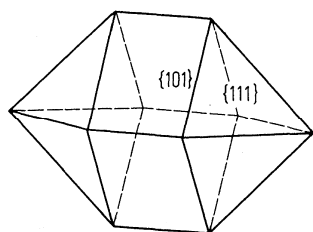
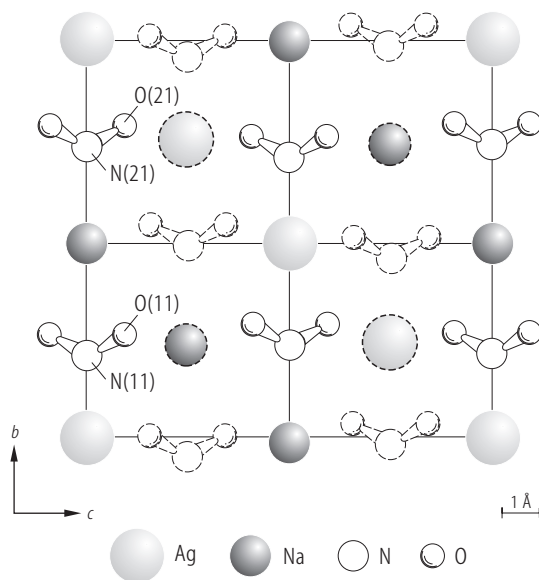
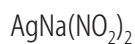


**Fig. 28A-2-001.**  $\text{AgNa}(\text{NO}_2)_2$ . Solubility curve for  $\text{AgNO}_2$ – $\text{NaNO}_2$ – $\text{H}_2\text{O}$  system [53Cav].  $T = 25\text{ }^\circ\text{C}$ . Thick curve: liquidus. Full circles which are joined with a thin line indicate the composition of a saturated solution and that of solid crystallized from it.



**Fig. 28A-2-002.**  $\text{AgNa}(\text{NO}_2)_2$ . Crystal form [53Cav].



**Fig. 28A-2-003.**  $\text{AgNa}(\text{NO}_2)_2$ . Structure of phase II [74Ish].  $T = 293\text{ K}$ . Projection along  $[100]$ . The hatched figures show the atoms by  $\approx a/4$  above (or below) the layer on which solid figures lie. The figure is drawn as the fully ordered state. For the population parameters, see Table 28A-2-004.

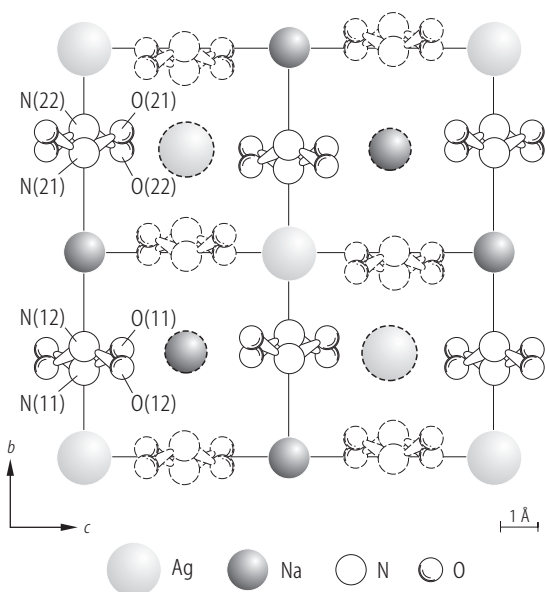
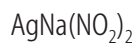


**Fig. 28A-2-004.**  $\text{AgNa}(\text{NO}_2)_2$ . Structure of phase I [74Ish].  $T = 323$  K. Projection along [100]. The hatched figures show the atoms by  $\approx a/4$  above (or below) the layer on which solid figures lie. For the population parameters, see Table 28A-2-004.

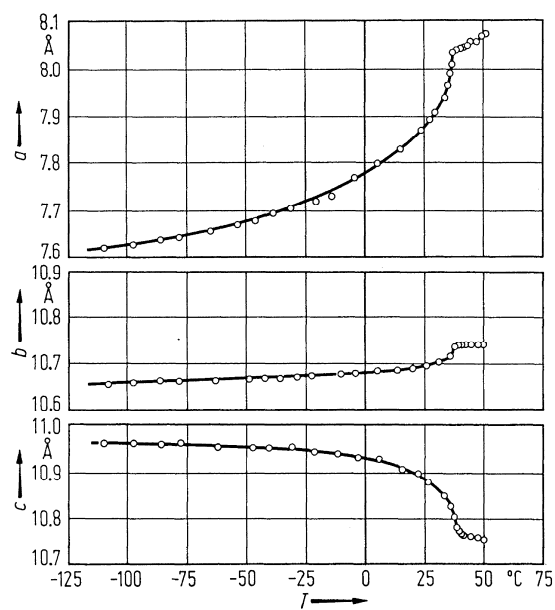


**Fig. 28A-2-005.**  $\text{AgNa}(\text{NO}_2)_2$ .  $a$ ,  $b$ ,  $c$  vs.  $T$  [71Mik].

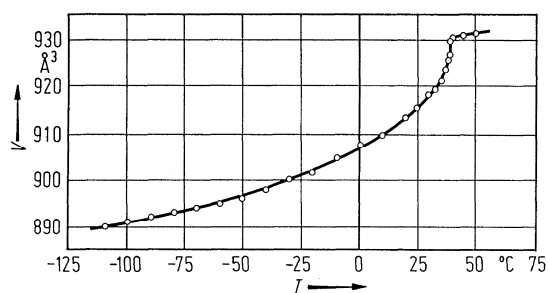


**Fig. 28A-2-006.**  $\text{AgNa}(\text{NO}_2)_2$ .  $V$  vs.  $T$  [71Mik].  $V$ : unit cell volume.

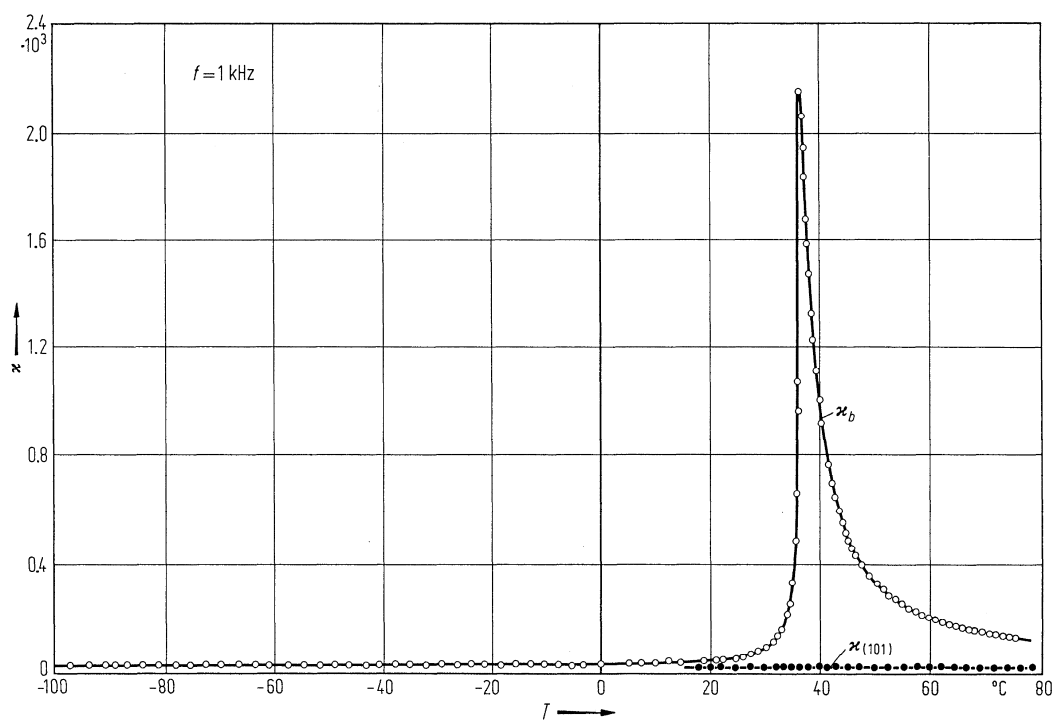


**Fig. 28A-2-007.**  $\text{AgNa}(\text{NO}_2)_2$ .  $\kappa_b$ ,  $\kappa_{(101)}$  vs.  $T$  [70Ges1].  $\kappa_{(101)}$ : dielectric constant perpendicular to the (101) plane.

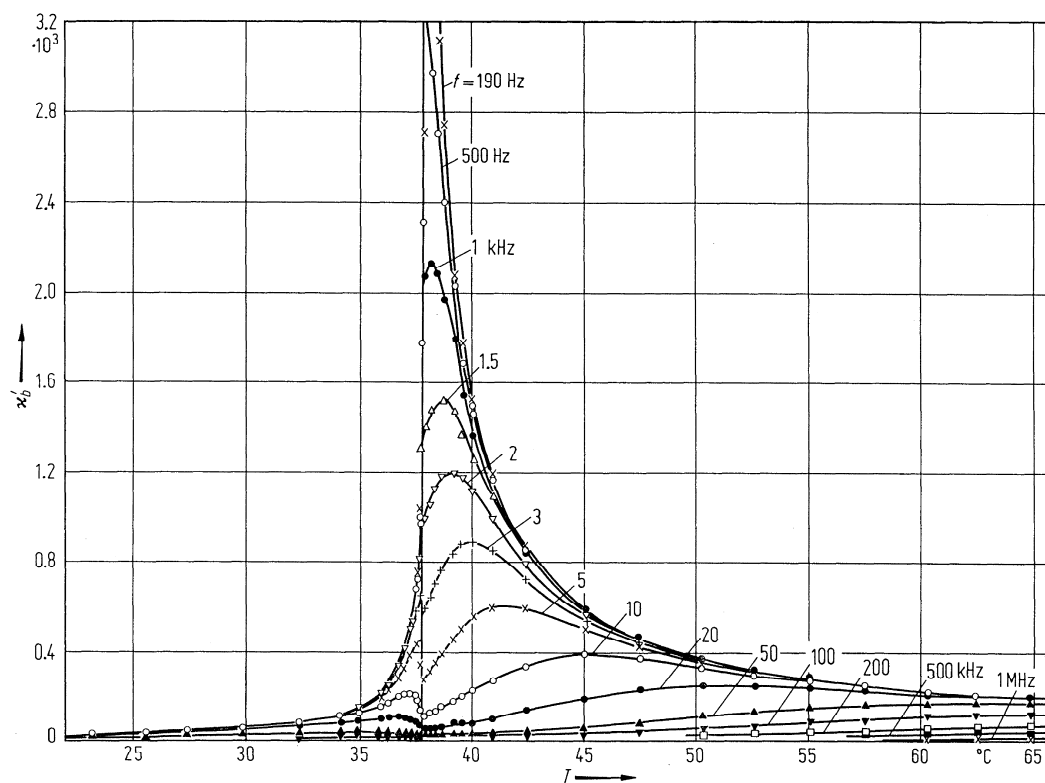


Fig. 28A-2-008.  $\text{AgNa}(\text{NO}_2)_2$ .  $\kappa'_b$  vs.  $T$  [72Ges1]. Parameter:  $f$ .

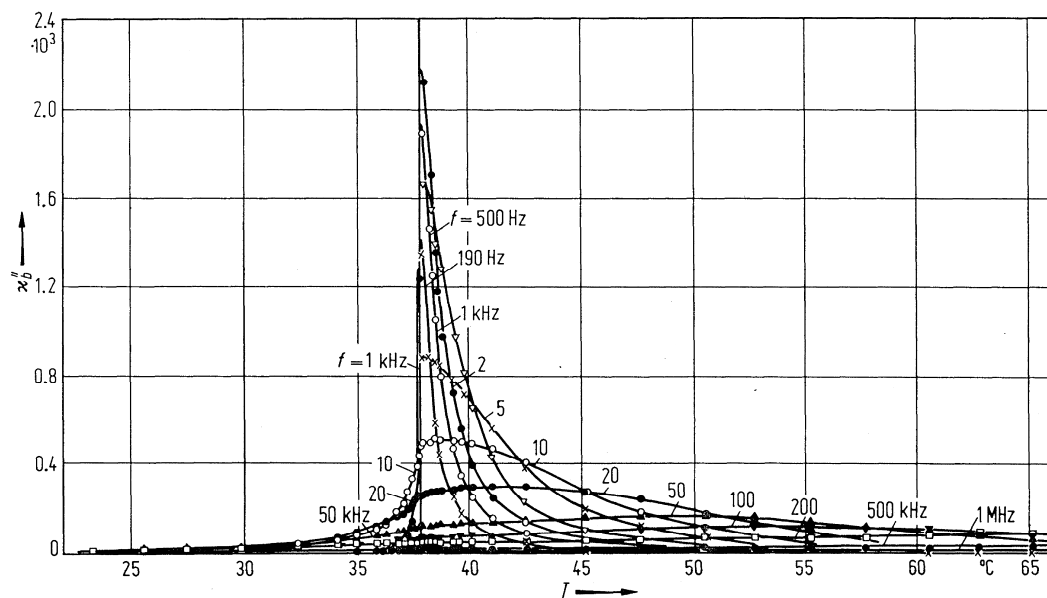
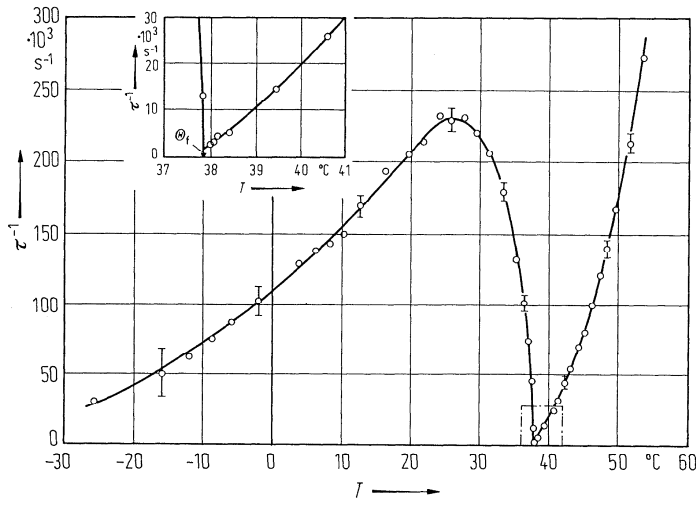
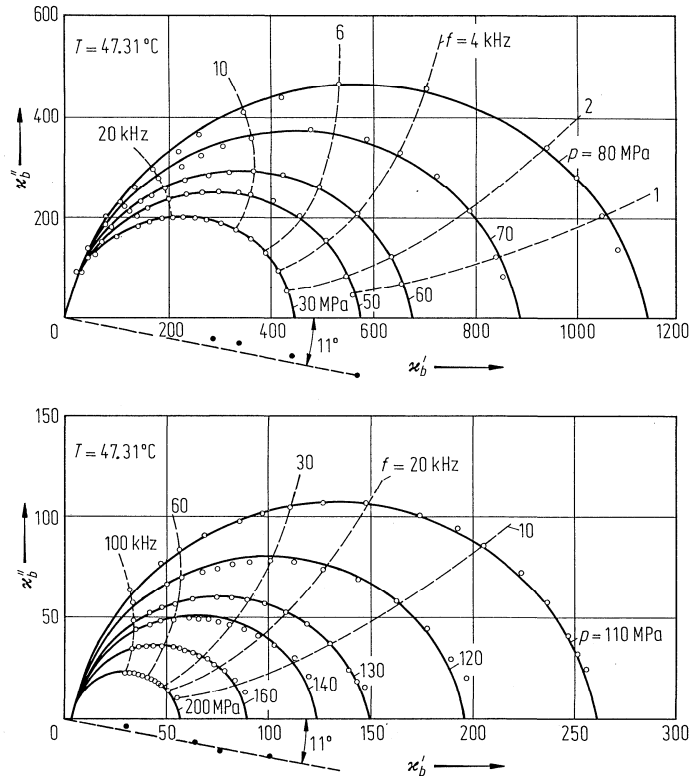


Fig. 28A-2-009.  $\text{AgNa}(\text{NO}_2)_2$ .  $\kappa''_b$  vs.  $T$  [72Ges1]. Parameter:  $f$ .



**Fig. 28A-2-010.**  $\text{AgNa}(\text{NO}_2)_2$ .  $1/\tau$  vs.  $T$  [76Gro].  $\tau$ : dielectric relaxation time.



**Fig. 28A-2-011.**  $\text{AgNa}(\text{NO}_2)_2$ . Cole-Cole diagrams of the complex dielectric constant,  $\kappa_b = \kappa'_b - i\kappa''_b$ , [80Pet].  $T = 47.31$  °C. Parameter:  $p$ .

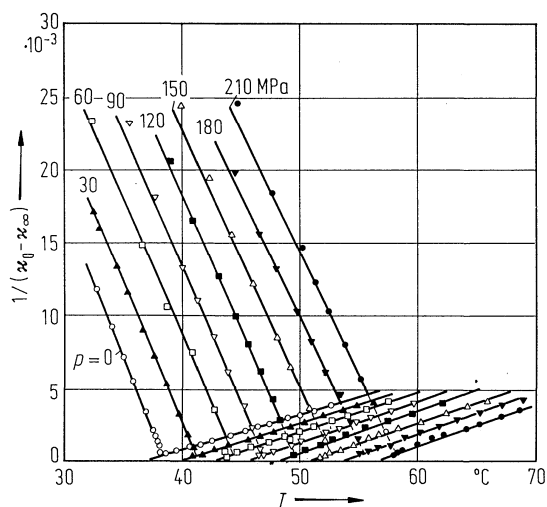


Fig. 28A-2-012.  $\text{AgNa}(\text{NO}_2)_2$ .  $1/(\kappa_0 - \kappa_\infty)$  vs.  $T$  [80Pet]. Parameter:  $p$ .  $\kappa_0$ : static dielectric constant along  $b$ .  $\kappa_\infty = 4.5$ .

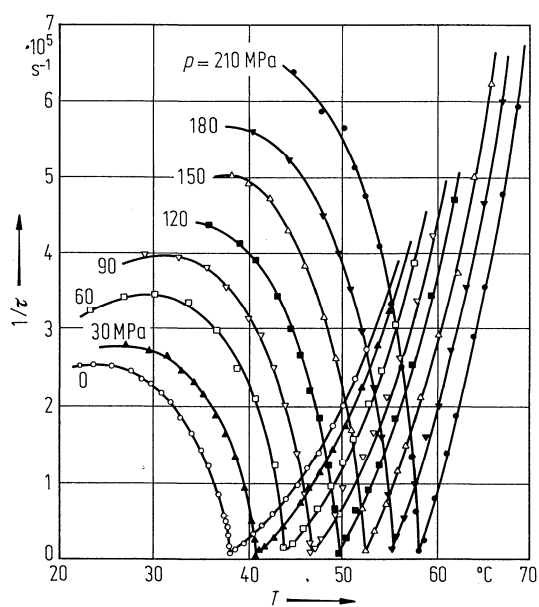


Fig. 28A-2-013.  $\text{AgNa}(\text{NO}_2)_2$ .  $1/\tau$  vs.  $T$  [80Pet]. Parameter:  $p$ .  $\tau$ : dielectric relaxation time.

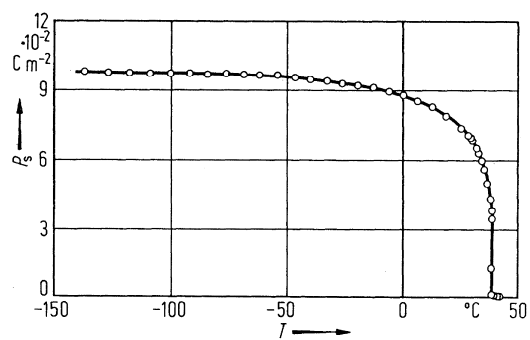
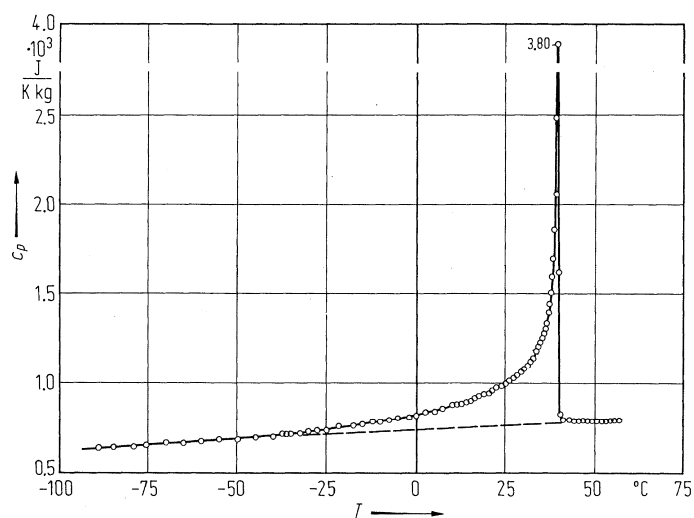
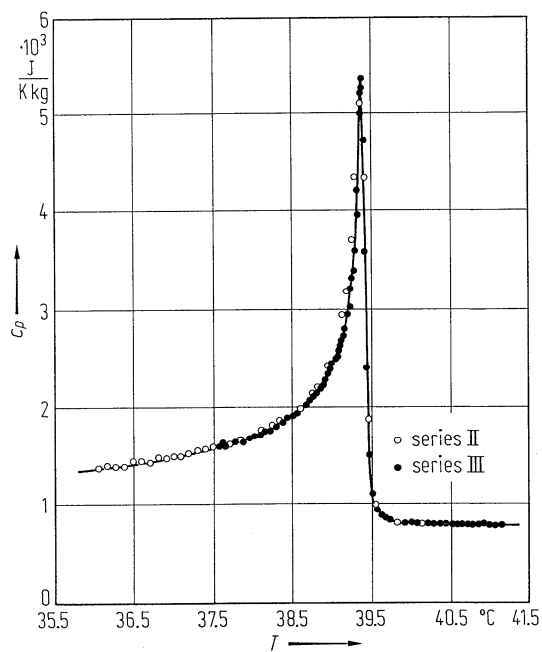


Fig. 28A-2-014.  $\text{AgNa}(\text{NO}_2)_2$ .  $P_s$  vs.  $T$  [72Ges3].



**Fig. 28A-2-015.**  $\text{AgNa}(\text{NO}_2)_2$ .  $c_p$  vs.  $T$  [77Hel].



**Fig. 28A-2-016.**  $\text{AgNa}(\text{NO}_2)_2$ .  $c_p$  vs.  $T$  in the vicinity of  $\Theta_{\text{II-I}}$  [77Hel]. Temperature increments of 0.1 K (series II) and 0.03 K (series III) were applied.

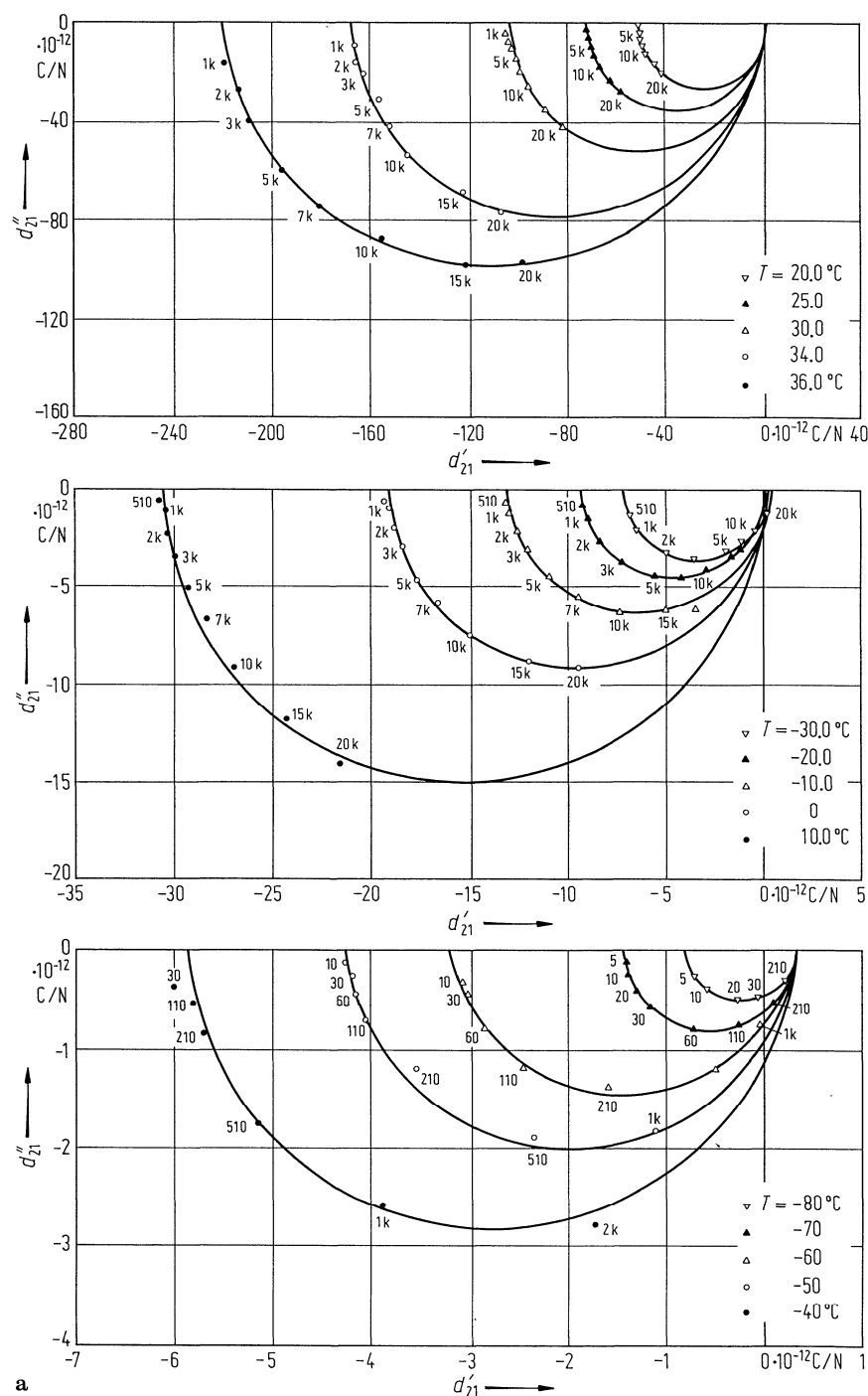


**Fig. 28A-2-017.**  $\text{AgNa}(\text{NO}_2)_2$ . Cole-Cole diagrams of complex piezoelectric constant,  $d_{2\lambda} = d'_{2\lambda} - id''_{2\lambda}$  [81Yam]. Parameter:  $T$ . (a)  $d_{21}$ , (b)  $d_{22}$ , (c)  $d_{23}$ .



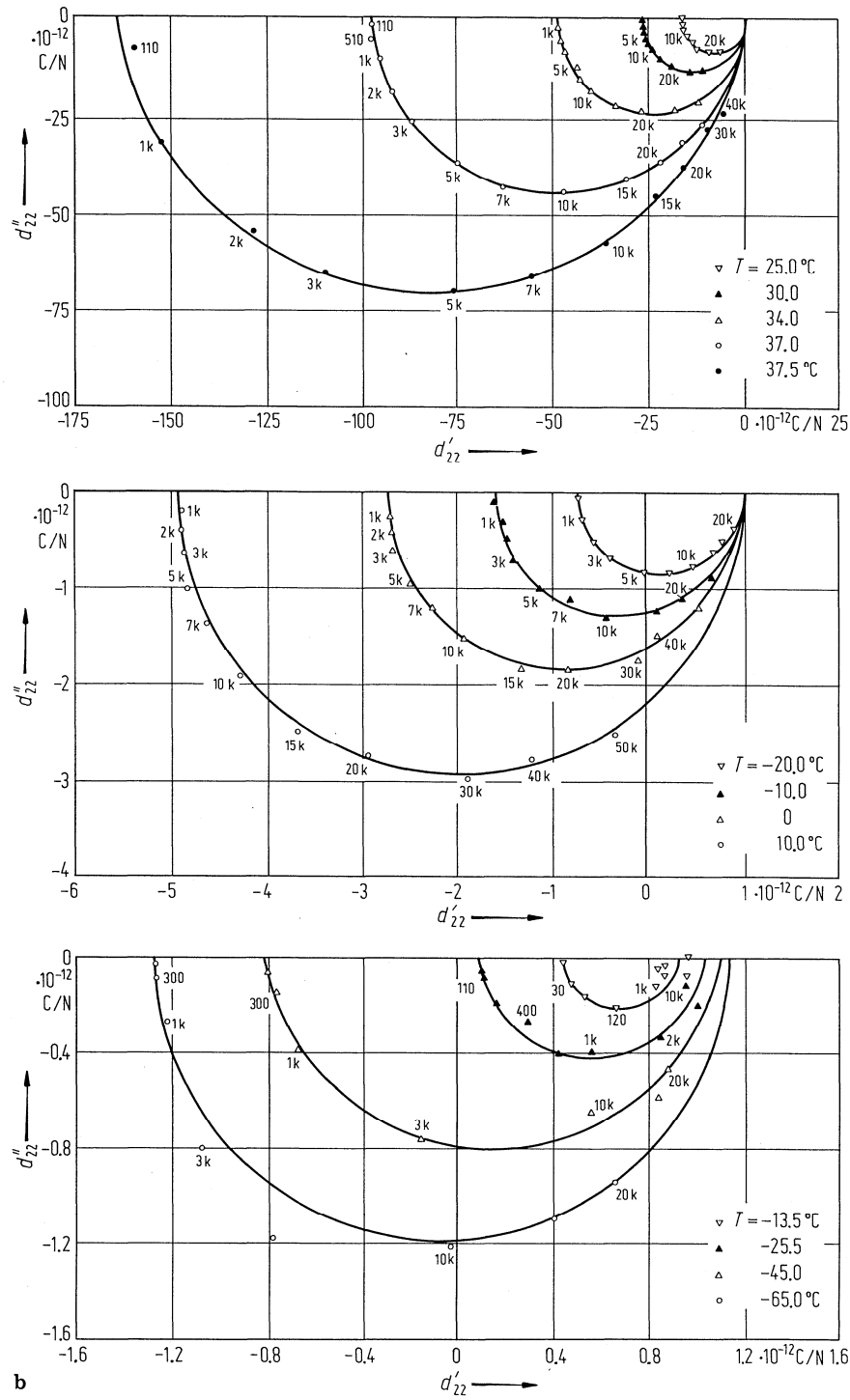


Fig. 28A-2-017b.

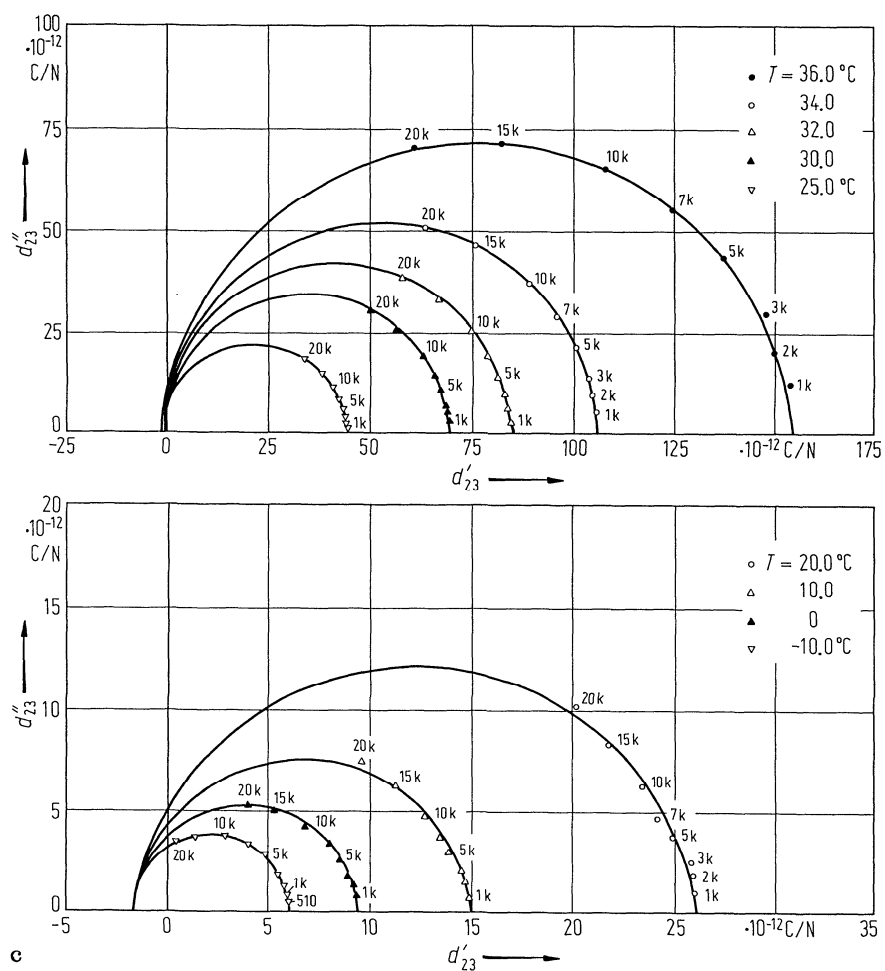
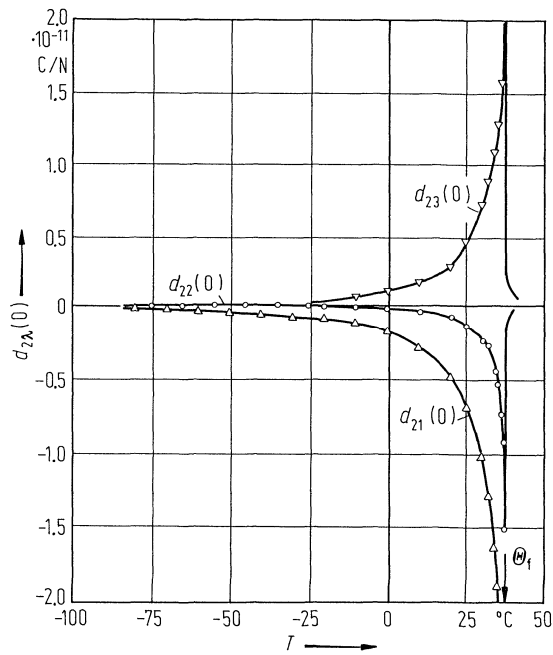
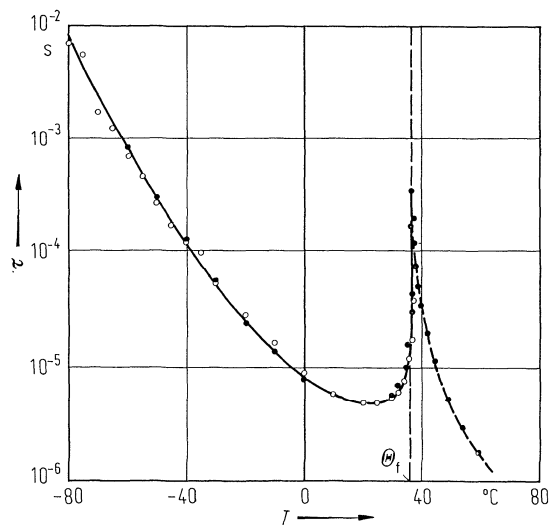


Fig. 28A-2-017c.



**Fig. 28A-2-018.**  $\text{AgNa}(\text{NO}_2)_2$ .  $d_{2\lambda}(0)$  vs.  $T$  [81Yam].  $d_{2\lambda}(0)$ : static piezoelectric constant.



**Fig. 28A-2-019.**  $\text{AgNa}(\text{NO}_2)_2$ .  $\tau$  vs.  $T$  [81Yam].  $\tau$ : piezoelectric (open circle) and dielectric (full circle) relaxation times.

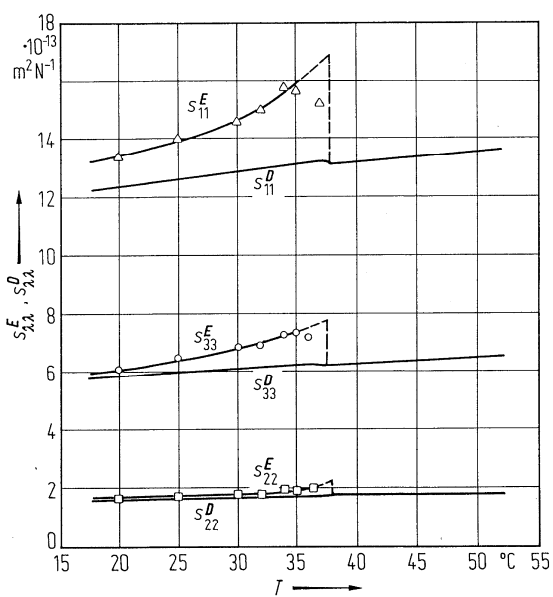


**Fig. 28A-2-020.**  $\text{AgNa}(\text{NO}_2)_2$ .  $s_{\lambda\lambda}^E, s_{\lambda\lambda}^D$  vs.  $T$  [79Yam].

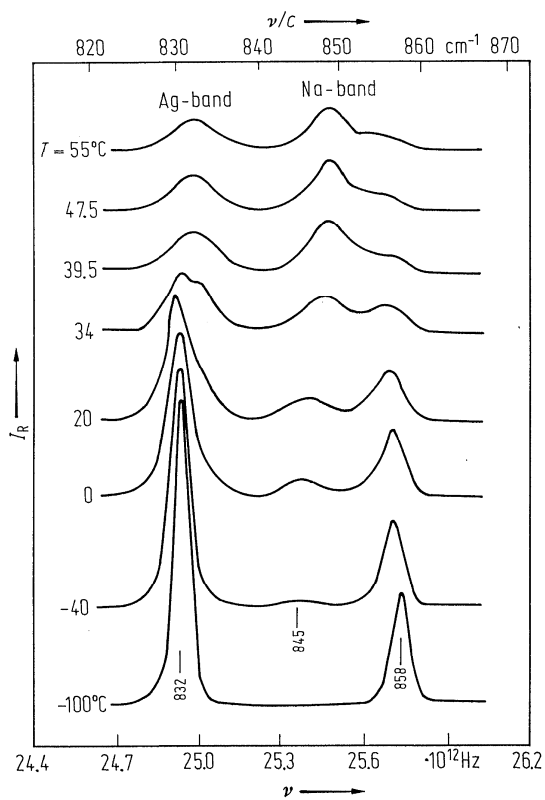


**Fig. 28A-2-021.**  $\text{AgNa}(\text{NO}_2)_2$ .  $I$  vs.  $\nu$  [80Han]. Parameter:  $T$ .  $\nu, I$ : frequency and intensity of Raman scattering of  $\nu_2$  vibrational modes of  $\text{NO}_2^-$  ions. Ag-band: absorption  $\text{NO}_2^-$ 's denoted (11) or (22), Na-band: absorption by  $\text{NO}_2^-$ 's denoted (12) or (21) in Fig. 28A-2-003 and Fig. 28A-2-004.

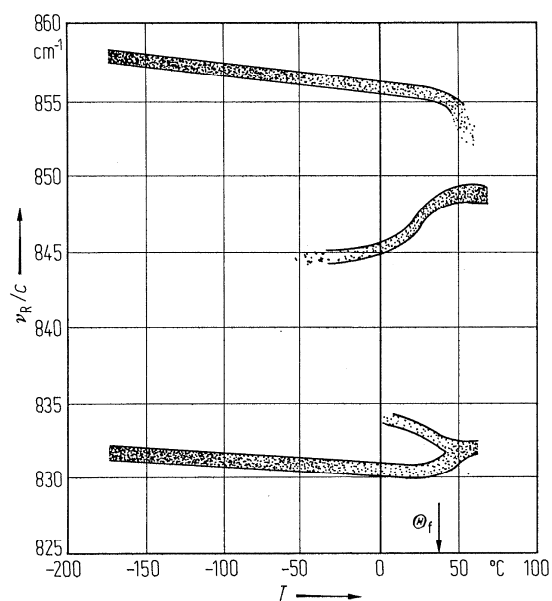


**Fig. 28A-2-022.**  $\text{AgNa}(\text{NO}_2)_2$ .  $\nu_R/c$  vs.  $T$  [80Han].  $\nu_R/c$ : wave number of Raman scattering of  $\nu_2$  vibrational modes of  $\text{NO}_2^-$  ions. See caption of Fig. 28A-2-021.

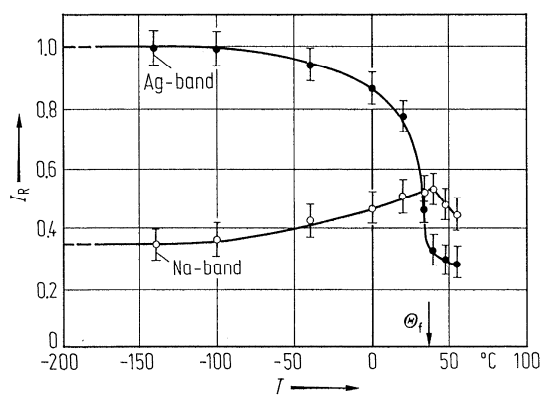


**Fig. 28A-2-023.**  $\text{AgNa}(\text{NO}_2)_2$ .  $I_R$  vs.  $T$  [80Han].  $I_R$ : intensity of Raman scattering of  $\nu_2$  vibrational modes of  $\text{NO}_2^-$  ions. See caption of Fig. 28A-2-021.

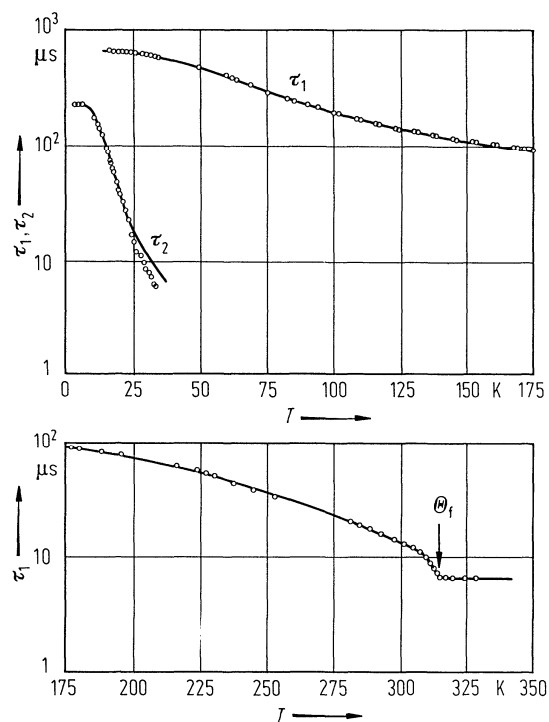


**Fig. 28A-2-024.** AgNa(NO<sub>2</sub>)<sub>2</sub>.  $\tau_1$ ,  $\tau_2$  vs.  $T$  [86Thy].  $\tau_1$ ,  $\tau_2$ : characteristic decay time of the laser induced luminescence  $I(t)$ .  $I(t)$ : induced luminescence expressed as  $I(t) = I_1 \exp(-t/\tau_1) + I_2 \exp(-t/\tau_2)$ . The lower figure shows the data in transition region [83Hap].

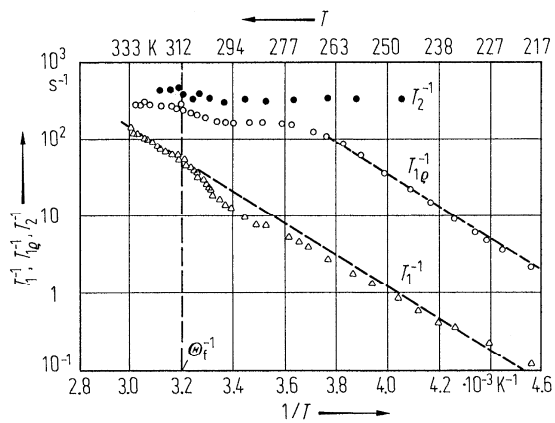


**Fig. 28A-2-025.** AgNa(NO<sub>2</sub>)<sub>2</sub>.  $1/T_1$ ,  $1/T_{1\rho}$ ,  $1/T_2$  vs.  $1/T$  for  $^{23}\text{Na}$  [78Gro1].  $f = 20$  MHz.

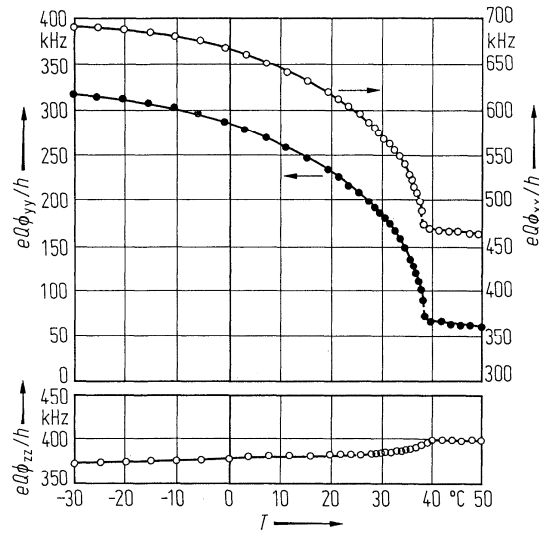


**Fig. 28A-2-026.**  $\text{AgNa}(\text{NO}_2)_2$ .  $eQ\phi_{ii}/h$  vs.  $T$  [78Gro2].  $eQ\phi_{ii}/h$ : principal values of the quadrupole coupling tensor of  $^{23}\text{Na}$ . In phase I,  $x \parallel a$ ,  $y \parallel b$ ,  $z \parallel c$ . In phase II,  $y \parallel b$ ,  $x$  and  $z$  make angles of  $\pm 4^{\circ}$  with the  $a$  and  $c$  axes, respectively.

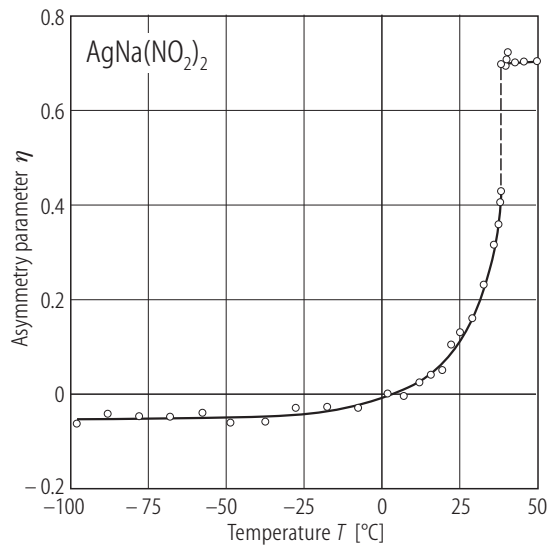


**Fig. 28A-2-027.**  $\text{AgNa}(\text{NO}_2)_2$ .  $\eta$  vs.  $T$  [73Hik].  $\eta$ : asymmetry parameter,  $\eta = (\phi_{22} - \phi_{33})/\phi_{11}$ .